Algorithms for Pavement Distress Classification by Video Image Analysis

J. ADOLFO ACOSTA, J. LUDWIG FIGUEROA, AND ROBERT L. MULLEN

A fundamental component of computer-based video image analysis for pavement distress evaluation is identification of the type of distress from geometric and textural properties of an area of interest identified during image analysis. This study describes the algorithms used to identify and classify the most common pavement distress types once a possible distress region is identified on an image. The classification is accomplished in three steps. First, geometric and textural features are calculated for a region of interest. Next, the features of that region are used to determine whether any other regions in an image are actually part of the same pavement distress. Finally, the extracted image features are used with a decision tree to identify the specific pavement distress type, its severity, and its extent. The features and decision trees have been tested on several thousand pavement images and the system that contains the decision tree has been used successfully by the Ohio Department of Transportation since May 1994.

Computer-based image analysis has become a major topic of research due to its broad application in almost all sciences, including pavement engineering. Identification and quantification of distress that can be measured by width, length, area, and in some cases by depth is made possible by automatic analysis of images captured by a computer from video or film recordings. Analysis of images to obtain a pavement rating based on the amount of distress is being developed at several universities and private companies.

Acosta (*1*) and Figueroa et al. (*2*) investigated different techniques for the automatic segmentation of concrete, asphalt concrete, and composite pavement images; thresholding of gray-level pictures using one- and two-dimensional entropy; and innovative techniques for the identification of cracks in textured media. In addition, they developed and evaluated another method, the vertical region segmentation (VRS), and they performed a preliminary cluster classification using several geometrical and statistical features computed for each cluster and extracted from the background. The reliability and accuracy of the methods employed in automatic segmentation and the distress classification were assessed.

A fundamental component of computer-based video image analysis for pavement distress evaluation is the identification of the type of distress from geometric and textural properties of the area of interest, which was identified during image analysis. This study describes the algorithms used in the identification and classification of the most common pavement distress types once a possible distress region is identified on an image. The classification is accomplished in three steps. First, geometric and textural features are calculated for a region of interest. Next, the features of a region are used to determine whether any other regions of an image are actually part of the same pavement distress. Finally, the extracted image features are used with a decision tree to identify the specific pavement distress type. In the following section a brief review of image processing is given first. Following this review, the definition of 19 features that were found to be required for identification of pavement distress types are defined. The procedure for making connections between neighboring clusters and the decision tree for determining the type, severity, and extent of pavement distress are presented.

J. A. Acosta, Resource International, Inc., Westerville, Ohio 43081. J. L. Figueroa and R. L. Mullen, Department of Civil Engineering, Case Western Reserve University, Cleveland, Ohio 44106.

IMAGE PROCESSING OVERVIEW

Computer-based image analysis was originally developed as a powerful tool in the medical sciences (*3,4*). Since then, its use has been extended to a variety of disciplines, as shown by several texts on digital image processing (*5,6*).

The general concept behind the image-processing approach of this study can be illustrated by explaining the five steps needed for image analysis: image digitization, image filtering or segmentation, clustering, feature extraction, and cluster classification.

The image digitization is accomplished through an image capturing board residing in the computer. The analog signal from a videotape player is transformed into a two-dimensional array of pixel elements in which each element has a value proportional to its brightness. The range of values of the array (the gray-level) typically varies from 0 (black) to 255 (white).

The image filtering is done by adaptive techniques using convolution, histogram, and primal sketch methods (*7–10*). It consists of separating the pixels belonging to the foreground (objects of interest) from those of the background.

The VRS method developed by Acosta (*1*) and Acosta et al. (*11,12*) is a statistical approach to image segmentation that is applied to pavement images, based on thresholds calculated by regression analysis. This method divides the image in narrow longitudinal (vertical) regions; each region is analyzed separately to minimize problems caused by a nonhomogeneous background or nonuniform illumination. The gray-level histogram is obtained to extract the gray-level average and the gray-level standard deviation (SD), taking into account only the gray levels with significant occurrences in the frequency distribution. Three zones are delimited: background, connective (possible), and foreground. The zones are distinguished based on two thresholds, s and t, obtained by regression analysis (Figure 1):

Q_1: True-foreground zone
Q_2: Possible-foreground zone
Q_3: True-background zone

An extension of this method was developed by Acosta (*13*) and Acosta et al. (*14*) that improves the detection of longitudinal cracks by also applying horizontal region segmentation (HRS). The

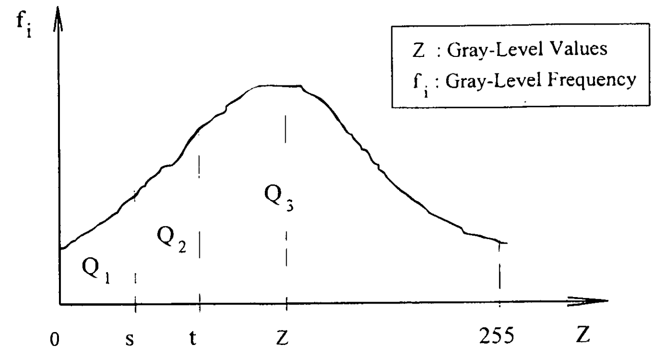

FIGURE 1 VRS zones.

improved method consists of tracing horizontal regions across the vertical regions described above, and analyzing each region separately, similar to the analysis of the vertical regions. Thresholds s^H and t^H are obtained and the pixels in the region are assigned to zones Q_1^H, Q_2^H, or Q_3^H, depending on their gray-level value, as follows:

Q_1^H: True-foreground zone from HRS
Q_2^H: Possible-foreground zone from HRS
Q_3^H: True-background zone from HRS

Pixels are pre-identified as background, Q_b and foreground, Q_f. They are designated as pre-identified because in the clustering procedure, clusters having a total number of pixels (both true-foreground and possible-foreground) less than a minimum value p and those with a number of possible-foreground pixels less than a minimum value q are automatically eliminated from further consideration. The improvement essentially consists of applying region segmentation in both directions, when needed, or combining both the VRS and the HRS methods into vertical and horizontal region segmentation VHRS. Adjacent areas of interest that were highlighted by filtering are clustered to and from objects.

Once an object in the image is found, geometric and statistical properties related to shape and gray level are calculated (feature extraction). From the information extracted, using appropriate guidelines, the object can be classified (cluster classification) as pavement distress, pavement feature, or unknown object (litter, debris, etc.). Pavement is then rated by applying the dimensional guidelines specified by the rating procedure.

This paper specifically addresses the rules necessary for cluster classification applied to pavement distress analysis, using properties obtained during feature extraction. Detailed discussions of other aspects required in image processing for pavement distress and condition evaluation can be found in Acosta (*13*) and Acosta et al. (*14*).

FEATURE EXTRACTION

Feature extraction reduces a region on an image to a limited number of geometric or textural properties. Certain features are selected that provide the capability of distinguishing between the different classes of pavement distress types. More than 50 preliminary features were chosen and extracted from a representative sample of images. The output values were analyzed and the features that best characterized the types of distress were adopted as the final features to be used in the pavement distress analysis.

A digitized image after contrast enhancement can be defined by:

$$I^* = \{f^*(x, y) \mid (0 \le x \le M) \wedge (0 \le y \le N)\} \tag{1}$$

$$Z_{\min} \le f^*(x, y) \le Z_{\max} \tag{2}$$

$$f^*(x, y) = \frac{f(x, y) - \rho_{\min}}{\rho_{\max} - \rho_{\min}} \times (Z_{\max} - Z_{\min}) \tag{3}$$

where:

$f^*(x, y)$ = gray level value (after transformation) of pixel at (x,y) coordinates;
M, N = number of rows and columns in image;
$\rho_{\min}, \rho_{\max}$ = maximum and minimum gray level values in image; and
$Z_{\min}$ = 0 and $Z_{\max}$ = 255 (minimum and maximum values in gray scale).

For a situation in which b_{ij} is the characteristic function of the cluster O_k such that:

$$b_{ij} \begin{cases} = 1 \text{ if } f^*(i,j) \in Q_f \wedge f^*(i,j) \in O_k \\ = 0 \text{ if otherwise} \end{cases} \tag{4}$$

Where Q_f is defined as follows:

$$Q_f = \{f(x, y) = z \mid z \in (Q_3 \cup Q_3^H)\} \tag{5}$$

The following geometric features are defined:

- Cluster area: number of pixels forming the cluster.

$$A = \sum_i \sum_j b_{ij} \tag{6}$$

- Aspect ratio: ratio between sides of a bounding box enclosing the cluster (Figure 2).

$$SF = \frac{\Delta_y}{\Delta_x}$$

$$\text{where } \Delta_y = y_{\max} - y_{\min} \text{ and } \Delta_x = x_{\max} - x_{\min} \tag{7}$$

- Angle of principal moments of inertia: angle of principal moment of inertia with respect to the horizontal, obtained from the following equations.

$$\tan 2\Theta = \frac{2I_{\bar{x}\bar{y}}}{I_{\bar{y}} - I_{\bar{x}}} \tag{8}$$

where

$$I_{\bar{x}} = I_x - \frac{P_x^2}{A}$$

$$I_{\bar{y}} = I_y - \frac{P_y^2}{A} \tag{9}$$

$$I_{\bar{x}\bar{y}} = I_{xy} - \frac{P_x P_y}{A} \tag{10}$$

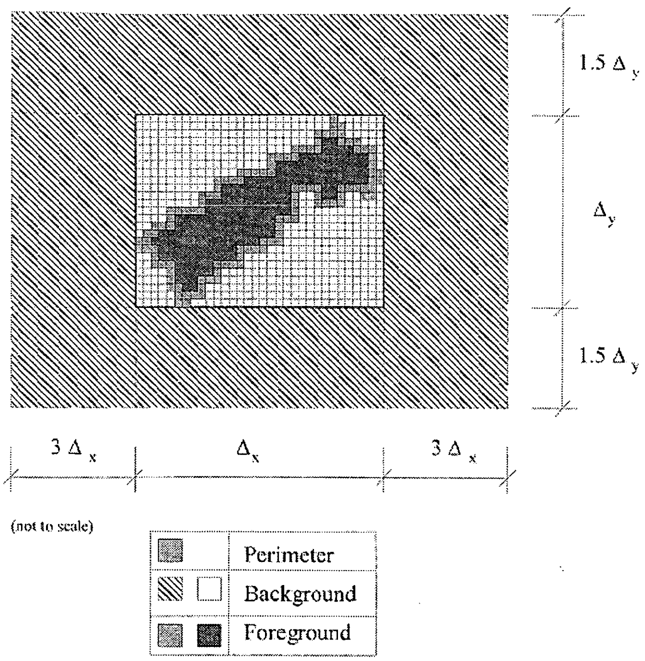

FIGURE 2 Foreground, perimeter, and background areas.

are the second moments of inertia (for both axes) and the product moment of inertia, respectively.

$$P_x = \sum_i \sum_j y \cdot b_{ij} \qquad P_y = \sum_i \sum_j x \cdot b_{ij} \tag{11}$$

are the first moments of area about the image coordinate axes, and

$$I_x = \sum_i \sum_j y^2 \cdot b_{ij}$$

$$I_y = \sum_i \sum_j x^2 \cdot b_{ij} \tag{12}$$

$$I_{xy} = \sum_i \sum_j xy \cdot b_{ij} \tag{13}$$

are the moments of inertia and the product moment of inertia, respectively.

- Coordinates of the center of gravity:

$$x_{cg} = \frac{P_x}{A}$$

$$y_{cg} = \frac{P_y}{A} \tag{14}$$

- Inertia ratio is calculated (*15*) as follows:

$$IR = \frac{I_{\max}}{I_{\min}} \tag{15}$$

where

$$I_{\max}, I_{\min} = \frac{I_{\bar{x}} + I_{\bar{y}}}{2} \pm \sqrt{(I_{\bar{x}} - I_{\bar{y}})^2 + 4\,(I_{\bar{x}\bar{y}})^2} \tag{16}$$

are the principal moments of inertia.

- Density: the ratio between the cluster's number of pixels and the area of the box enclosing the cluster.

$$D = \frac{A}{\Delta_y \times \Delta_x} \tag{17}$$

- Ratio between the number of possible-foreground and true-foreground pixels:

$$MTPR = \frac{\sum f_i \in (Q_2 \cup Q_2^H)}{\sum f_i \in Q_f} \tag{18}$$

- Cluster length along the angle Θ, L: obtained by scanning the cluster in the Θ direction.
- Average width:

$$W = \frac{A}{L} \tag{19}$$

- Ratio between length and width:

$$LWR = \frac{L}{W} \tag{20}$$

- Gray-level average:

$$\mu = \frac{\sum_i \sum_j f_{ij}}{A} \tag{21}$$

- Gray-level standard deviation:

$$\sigma_z = \frac{\sum (\mu_i - \mu)^2}{A} \tag{22}$$

- Perimeter, P, and perimeter area, A_p: calculated by scanning the cluster and adding up the number of pixels from its perimeter (Figure 2).
- Perimeter gray-level average: average of gray-level values of perimeter pixels f_{ij}^p

$$\mu_p = \frac{\sum_i \sum_j f_{ij}^b}{A_p} \tag{23}$$

- Background gray-level average: an area around the cluster was set as shown in Figure 2, and the gray-level values corresponding to pixels residing in this area were averaged.

$$\mu_b = \frac{\sum_i \sum_j f_{ij}^b}{A_b} \tag{24}$$

- Perimeter foreground ratio: ratio between the perimeter area and the foreground area, as follows.

$$PFR = \rho = \frac{A_p}{A} \tag{25}$$

- Squareness constant, K_s: calculated from above expression, for a rectangle as follows.

$$\rho = \frac{2\,(W + L)}{W \times L} \tag{26}$$

then

$$K_s = \frac{\rho\, WL}{W + L} = 2 \tag{27}$$

- Roundness constant, K_r: from Equation 25, for a circle, if D is the diameter:

$$\rho = \frac{\pi D}{\pi D^2} = \frac{4}{D} \tag{28}$$

then

$$K_r = \rho D = \rho L = 4 \tag{29}$$

- Square perimeter factor: obtained as the ratio between the cluster perimeter and the perimeter of a rectangle.

$$SPF = \frac{P}{2L + 2W} \quad \begin{cases} \text{Rectangle} \cong 1 \\ \text{Circle} \cong 0.79 \end{cases} \tag{30}$$

- Background-foreground gray-level ratio: ratio between the average gray-level of background pixels (Figure 2) and the cluster pixels.

$$BFGLR = \frac{\mu_b}{\mu_f} \tag{31}$$

The previously defined 19 features (Equations 4–31) were found to be sufficient to identify and quantify the severity and extent of all pavement distress types considered.

CLUSTER CONNECTION AND CLASSIFICATION

Prior to the final classification of a selected region on an image, a neighbor cluster connection was implemented to facilitate the identification of cracks during classification. The cluster is scanned along its perimeter to find adjacent clusters. In the event a neighboring cluster is detected, some properties (extracted features) are compared. If they satisfy the conditions imposed, they are merged to form a single cluster. The procedure continues until all clusters are scanned and compared with their neighbors.

For a case in which cluster k is being scanned and cluster l is found as a neighbor,

if $(\Theta_k \approx \Theta_l \approx \Theta_{kl}) \wedge (LWR_k \approx LWR_l)$ then clusters k and l are merged

where:

Θ_k, Θ_l = Angle of principal moment of inertia
Θ_{kl} = Average between angles Θ_k and Θ_l
LWR_k, LWR_l = Ratio between cluster length and cluster width

Following the cluster (neighbor) connection, the features described above are calculated for the new clusters so that they can be classified as one of the distress types included in the pavement condition rating (PCR) manual (*16*) or discarded from further analysis if they are nondistress.

The classification is performed in five main stages: depth-related cluster classification, cluster preliminary identification, cluster identification, cluster preclassification, and final classification. A description of the stages is given in the following sections, taking into account the distresses found in flexible, composite, and jointed portland cement concrete pavements.

Depth-Related Cluster Identification (Figure 3)

Flexible and Composite Pavements

The transverse depth is checked every 18 ft to verify the existence of rutting. Rutting is considered when it is greater than 0.1 in. The existence of corrugations is detected if five consecutive longitudinal readings indicating unevenness of pavement surface in the longitudinal profile greater than 0.1 in. are obtained. The readings are considered 18 ft apart.

Jointed Pavements

The existence of faulting is detected if a longitudinal unevenness greater than 0.1 in. is obtained. The readings are considered 18 ft apart.

Both transverse and longitudinal depth readings are obtained from ultrasonic devices that measure for rutting, corrugation, and faulting. These readings are directly encoded on the videotape using a gray-level scale for easy decoding during the analysis of individual frames, as described by Acosta (*13*) and Acosta et al. (*14*). Similarly, the longitudinal length is also continuously encoded on tape from readings obtained with a distance measuring instrument. The transverse length remains constant because the camera height and focus remain constant.

Cluster Preliminary Identification (Figure 4)

Six parameters that are helpful in the preliminary identification of the cluster, regardless of the type of pavement, are obtained based on the features extracted from the cluster.

- Longitudinal unevenness:
  Significant — Longitudinal reading > 0.2 in.
  Not significant — Otherwise
- Location (Figure 5):
  In road edge zone
  In wheel track zone
  In corner break zone on left side of lane or on right side of lane
- Shape factor:
  Longitudinal shape factor (SF) — $SF > 2$
  Transverse shape factor — $SF < 0.5$
  Normal shape factor — Otherwise
- Squareness:
  Semisquare — $K_s < 3$ and $K_r < 10$
  Not semisquare — Otherwise
- Size:
  Small — $A < 30$ in.^{2}
  Medium — $A > 30$ in.^{2} and $A < 60$ in.^{2}
  Large — Otherwise
- Darkness with respect to background:
  Dark — $BFGLR < 2.$
  Not dark — Otherwise

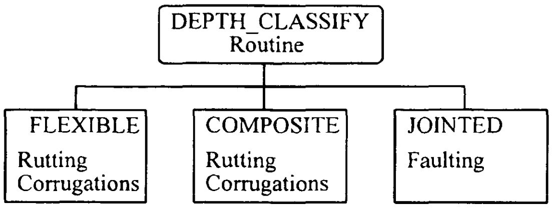

FIGURE 3 Depth-related cluster identification.

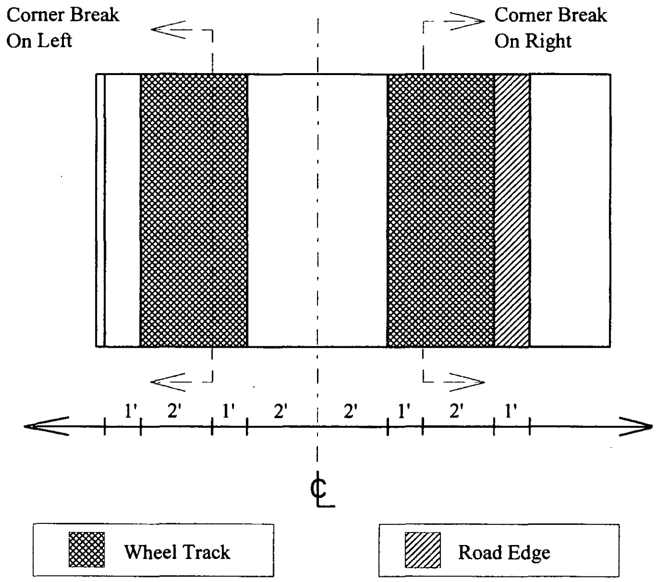

FIGURE 5 Roadway zones.

Cluster Identification

The cluster is identified based on the preliminary identification and additional features extracted from the object. Figure 6 shows the hierarchical top-down rule-based identification performed on the cluster.

Cluster Preclassification

In this stage, the cluster is preclassified as one of the distress types, considering the type of pavement being analyzed. Figures 7, 8, and 9 present the cluster preclassification for flexible, composite, and jointed pavements, respectively.

Cluster Final Classification

The distress types preclassified and marked by an asterisk (*) in Figures 8 and 9 are further analyzed in this stage, either to identify new distress types or to validate their classification. These figures show that only clusters in composite and jointed pavements need to be processed. Figures 10 and 11 present the steps followed in the cluster final classification for these two types of pavements, respectively. Figure 12 shows the scanned areas close to cracks in the final classification stage to verify the presence of joints and crack-related distress referenced in Figures 10 and 11.

Calculation of Severity and Extent Parameters

Once the cluster is classified, its quantification in terms of severity and extent has to be determined. Guidelines included in the PCR rating procedure (*16*) were followed in the implementation. The analysis program outputs a file containing the information needed to calculate the PCR value. This information corresponds to parameters such as average crack width, percentage of occurrence in section length, percentage of occurrence in section area, crack spacing, and so forth.

Different factors affect the estimation of the parameters needed for the distress quantification. Acosta (*13*) mentioned that the segmentation does not necessarily completely highlight the area

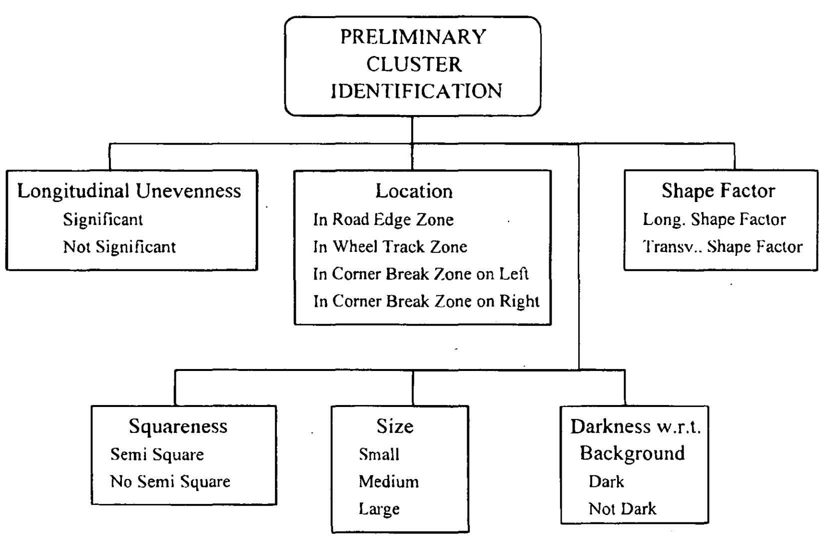

FIGURE 4 Preliminary cluster identification.

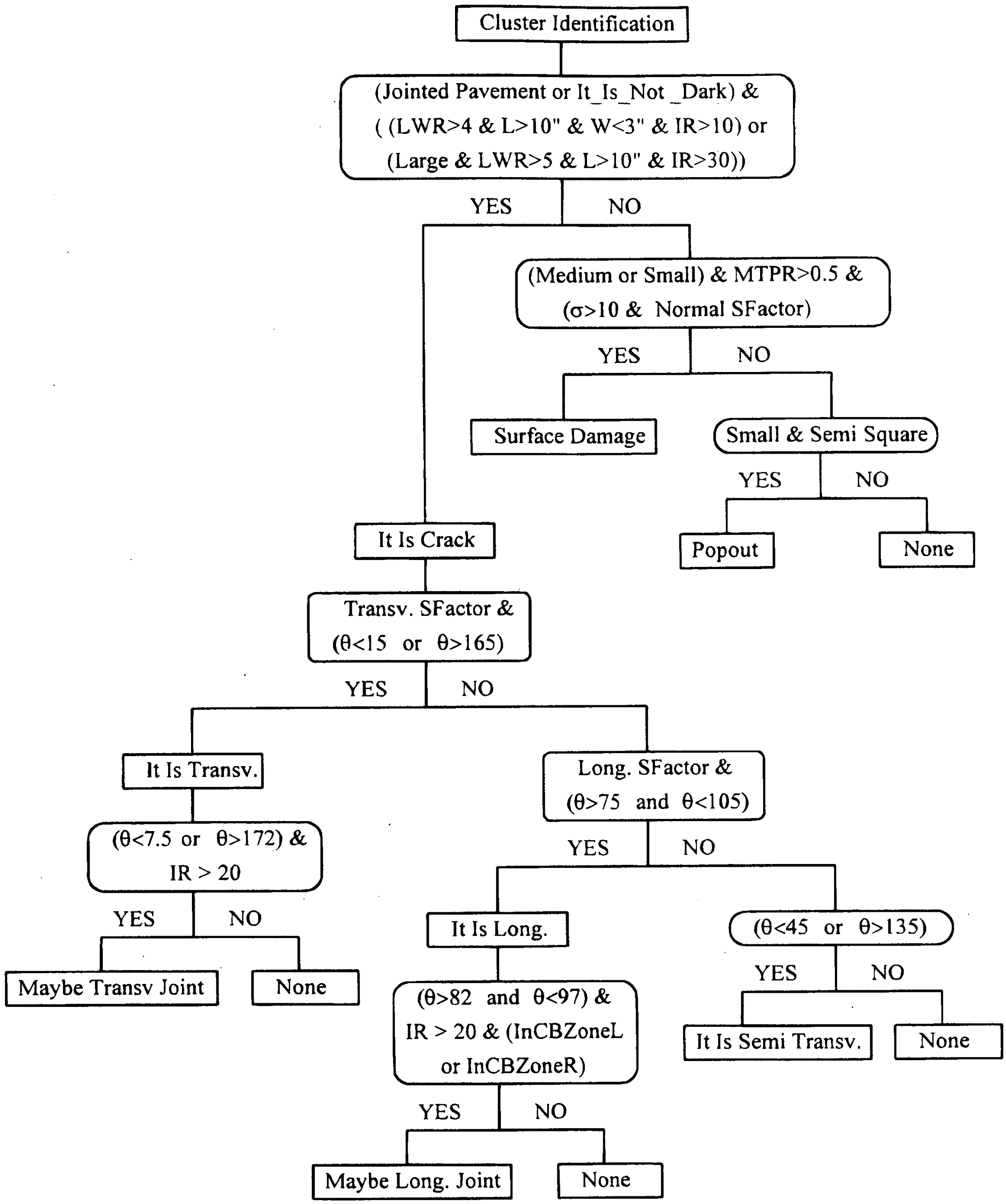

FIGURE 6 Cluster identification.

affected by the distress, and furthermore, it is necessary to estimate parameters spatially related. Consequently, there are two kinds of quantification parameters: local (e.g., crack width, crack length, etc.) and spatial (e.g., occurrence of single or multiple cracking, area affected by distress, etc.).

The estimation of local parameters is straightforward, whereas the estimation of spatial parameters requires additional work. Two data structures were implemented: distress information (*Distress-Info*) and distress region information (*Distress-Region-Info*) for the estimation of the severity and extent parameters. The image is subdivided into 18 in. × 18 in. regions, and each region is scanned to update the variables contained in the data structures that are to be used in the estimation of the spatial parameters.

The data structure variables are presented in the following tables.

Distress-Info

Acum. Cluster Area: summation of physical cluster area.
Acum. Length: summation of physical cluster length.
Acum. Area Affected: summation of area affected by distress.
Acum. Section Length Affected: summation of section length affected by distress.

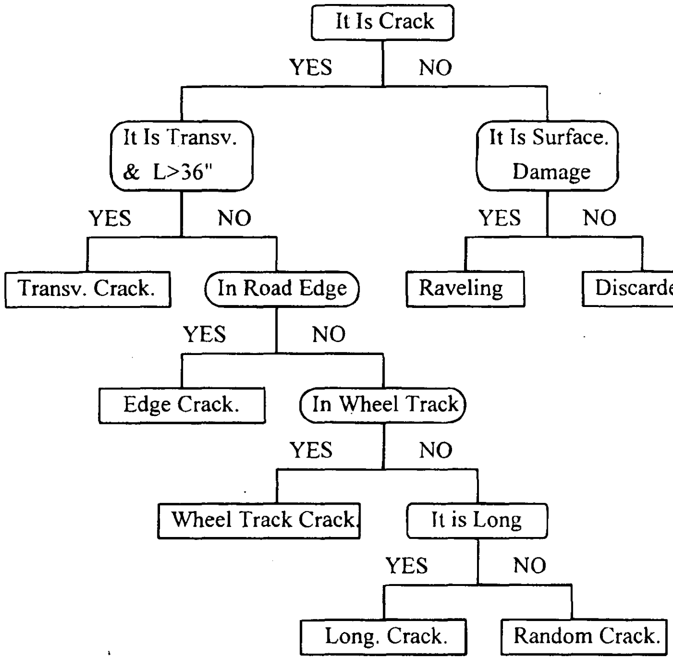

FIGURE 7 Cluster preclassification for flexible pavements.

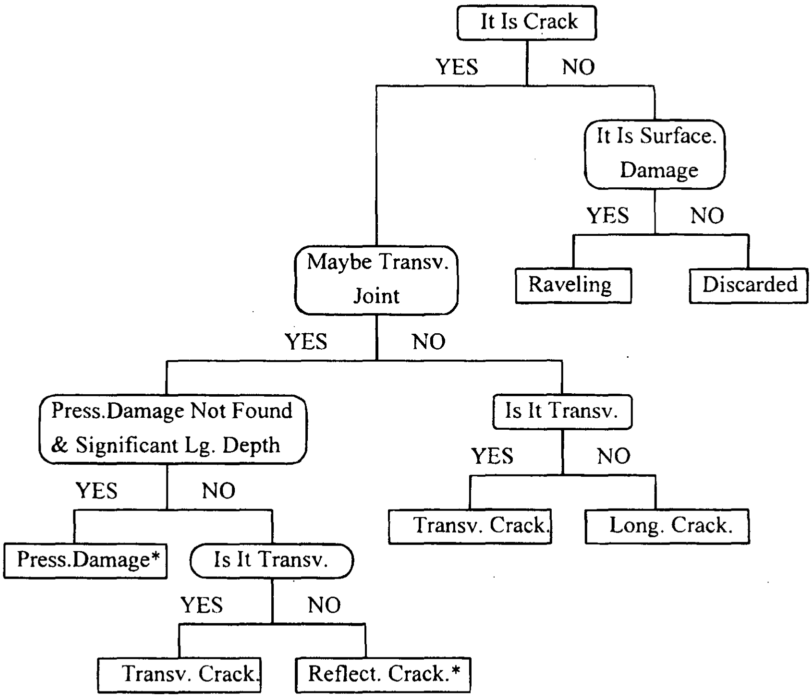

* Distress is further analyzed in the Final-Classification Stage.

FIGURE 8 Cluster preclassification for composite pavements.

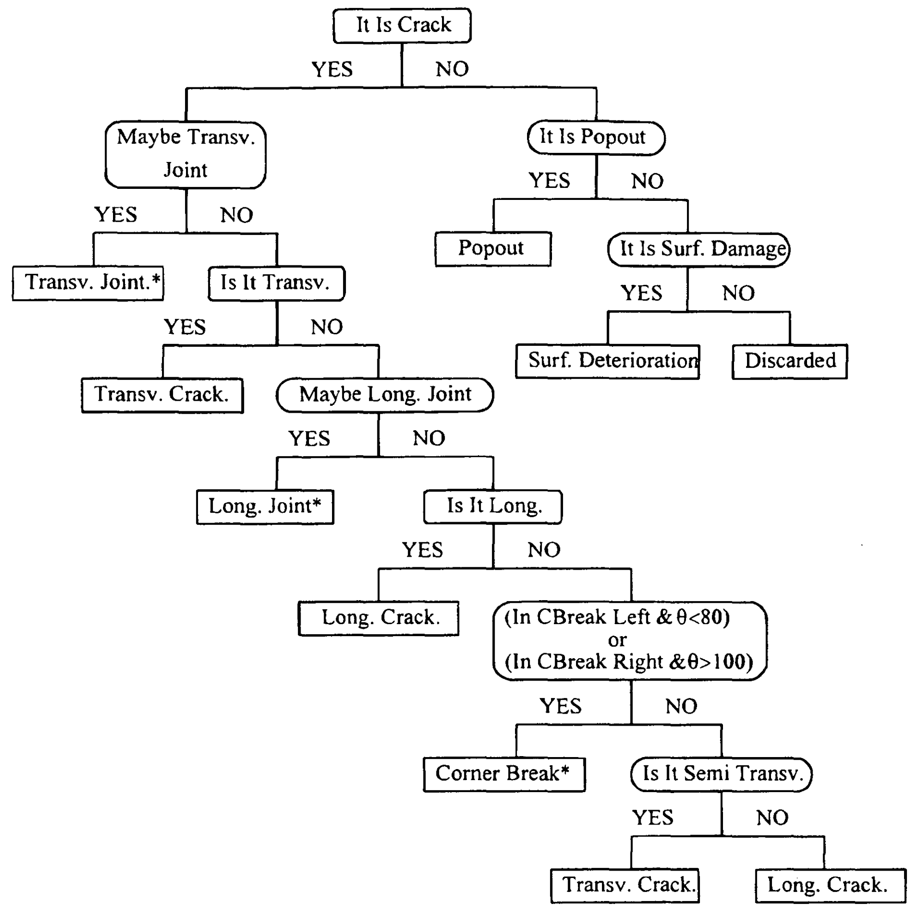

* Distress is further analyzed in the Final-Classification Stage.

FIGURE 9 Cluster preclassification for jointed pavements.

Acum. Depth: summation of depth reading (where applicable).

Acum. Gray-Level Std. Deviation: summation of standard deviations of gray-level values in clusters.

Acum. Number of Distresses: number of distresses identified in the section analyzed.

Acum. No. of Distress Region: summation of number of distresses in the region.

Number of Regions With Distress: summation of number of regions presenting the distress type.

Distress-Region-Info

Tot. No. of Pixels: total number of pixels belonging to the distress type.

No. of Distress Region: number of clusters classified under the distress type that is present in the region.

Note that for each distress type there are separate data structures, which contain the information mentioned above.

In summary, the procedure to estimate the parameters needed for the distress quantification follows three stages: local distress quantification, region distress quantification, and reporting of results for the analyzed section.

Local Distress Quantification

After the cluster is classified, the following variables are updated: Acum. Cluster Area, Acum. Length, Acum. Number of Distresses, Acum. Gray-Level Std. Deviation, and Acum. Depth (for depth-related distresses).

Region Distress Quantification

The following steps are performed in this stage:

- Count number of distress of each type in region,
- Update number of regions with distress for each type,
- Obtain area in the region in which each distress type occurs,
- Update the following equations:

$$\text{AcumAreaAffected} = \text{RegionArea} \times \frac{\text{DistressArea}_i}{\sum_i \text{DistressArea}} \quad (32)$$

$$\text{AcumLengthAffected} = \text{Region Length} \times \frac{\text{DistressLength}_i}{\sum_i \text{DistressLength}} \quad (33)$$

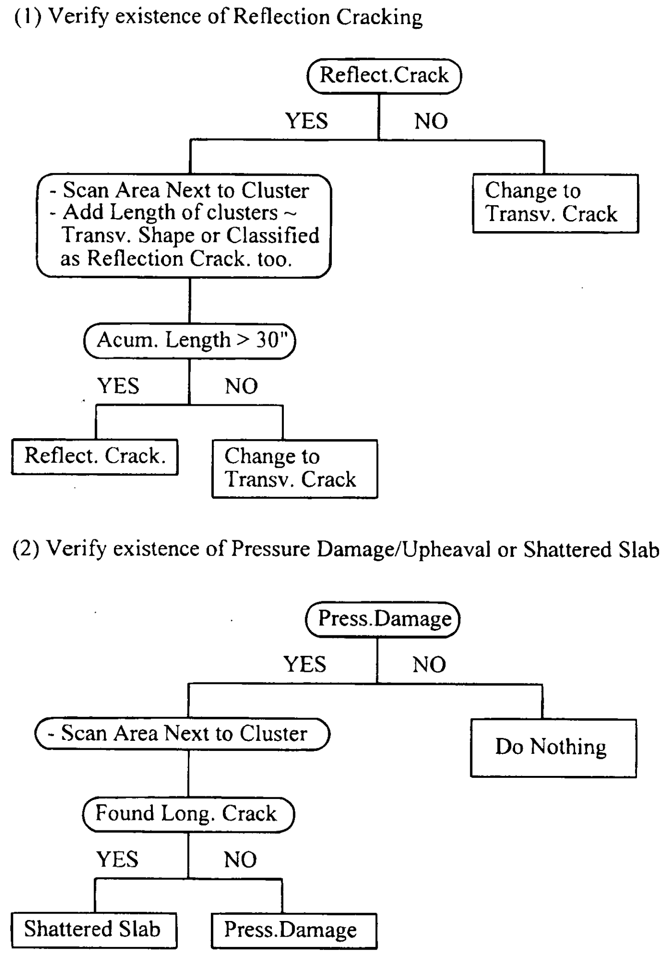

FIGURE 10 Cluster final classification for composite pavements.

This operation is performed only once, for regions within the same transverse location of the image.

Report of Results for Analyzed Section

The parameters needed for distress quantification in terms of severity and extent are obtained based on the values stored in the data structure: *Distress-Info*. They are summarized in the following equations.

- Average number of distresses per region:

$$\text{AveNDisPerReg} = \frac{\text{AcumNDisReg}}{\text{NRegWithDis}} \tag{34}$$

Useful in determining single or multiple cracking:

if (AveNDisPerReg $\leq$ 1), single otherwise, multiple.

- Average crack width:

$$\text{AveCrackWidth} = \frac{\text{AcumDisArea}}{\text{AcumLength}} \tag{35}$$

- Average distress length:

$$\text{AveDisLength} = \frac{\text{AcumLength}}{\text{AcumNDistress}} \tag{36}$$

- Average distress area:

$$\text{AveDisArea} = \frac{\text{AcumArea}}{\text{AcumNDistress}} \tag{37}$$

- Average gray-level SD:

$$\text{AveStdDeviation} = \frac{\text{AcumStdDev}}{\text{AcumNDistress}} \tag{38}$$

Useful in determining texture:

if AveStdDeviation $>$ 65 surface severely rough.
if 65 $<$ AveStdDeviation $>$ 25 open texture, medium roughness.
if AveStdDeviation $<$ 25 very little coarse aggregate.

- Percentage of occurrences per section area:

$$\text{PerOccSecArea} = \frac{\text{AcumAreaAffected}}{\text{SecArea}} \tag{39}$$

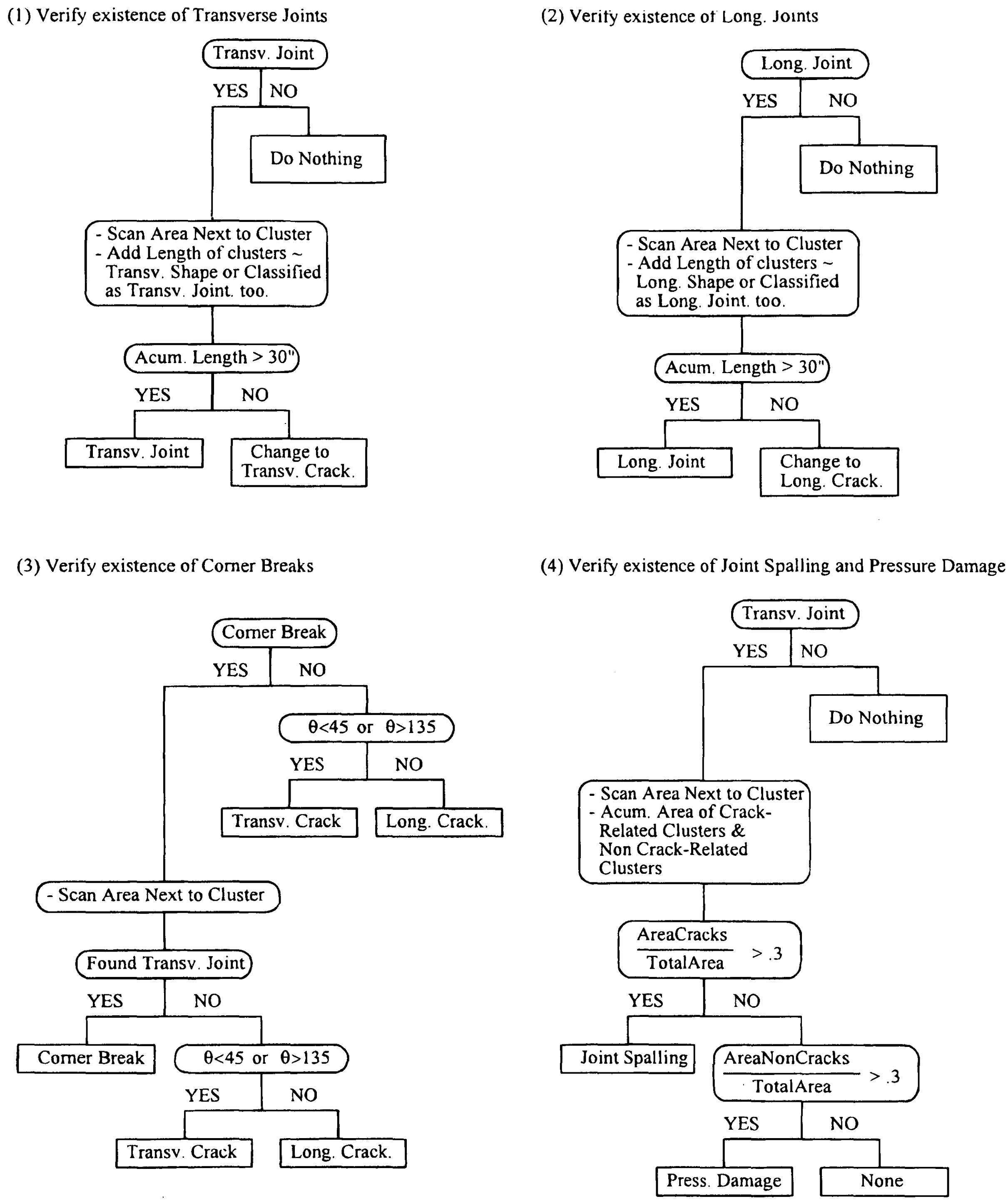

FIGURE 11 Cluster final classification for jointed pavements.

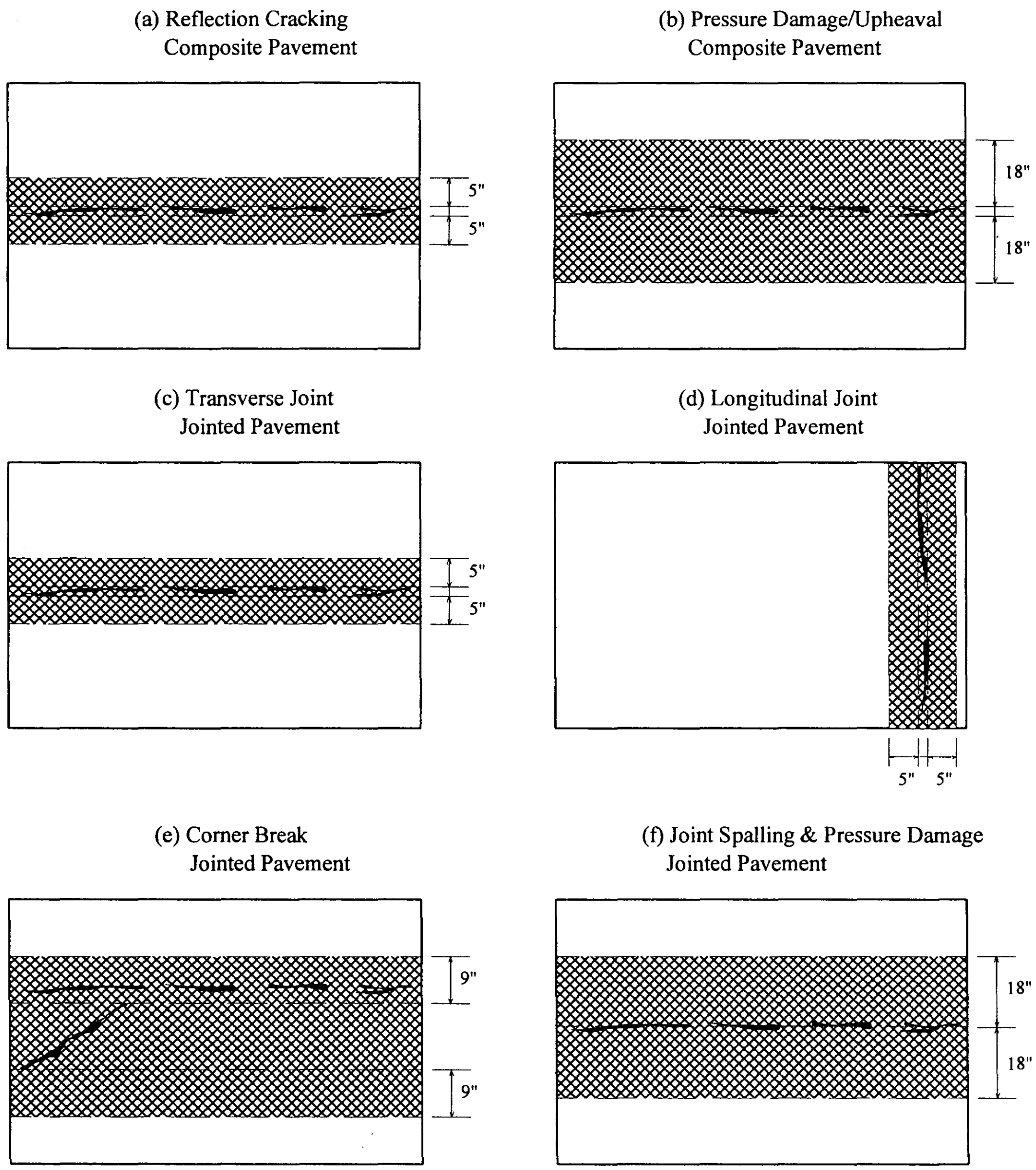

FIGURE 12 Scanned areas in final classification stage.

where SecArea = area of the section analyzed

- Percentage of occurrences per section length:

$$\text{PerOccSecLength} = \frac{\text{AcumSecLengthAffected}}{\text{SecLength}} \quad (40)$$

where SecLength = length of the section analyzed; or, in jointed pavements (where applicable):

$$\text{PerOccSecLength} = \frac{\text{AcumNDistress}}{\text{NSlabs}} \quad (41)$$

where NSlabs = number of slabs in the section analyzed.

- Average distress spacing:

$$\text{AveDisSpacing} = \frac{\text{SecLength}}{\text{AcumNDistress}} \quad (42)$$

- Average distress depth (for depth-related distresses):

$$\text{AveDisDepth} = \frac{\text{AcumDepth}}{\text{AcumNDistress}} \quad (43)$$

- Number of distress types per mile (where applicable in jointed pavements):

$$\text{AveDisDepth} = \frac{\text{AcumNDistress}}{\text{SecLength [miles]}} \quad (44)$$

TABLE 1 Comparison Between Manual and Automated PCR Values

Section	1	2	3	4
Length (meters)	5520	3685	4343	1931
Number of images	14,844	9,910	11,680	5,193
Data acquisition time. (min.)	4.12	2.75	3.24	1.44
Data processing time (min.)	41	27	32	14
Manual survey PCR	68.26	71.66	74.22	71.66
Automated survey PCR	65.10	72.20	75.30	71.70
% Difference of automated system with respect to manual values	-4.6%	0.8%	1.5%	0.06%

RESULTS

The distress classification system described herein was used to determine the PCR (*16*) for four pavement sections that were also rated by the Ohio Department of Transportation (ODOT). A summary of the manual and automated PCR is presented in Table 1. The images were collected using a vehicle, described by El Sanhouri (*13*), traveling at 80 km/hr (50 mi/hr). The collected video images were processed from videotape using a SUN Sparc-2 computer. As implemented, processing takes approximately 10 times as long as acquisition. The difference between manual and automated PCR is less than 5 percent in all test sections.

SUMMARY

Several methods have been proposed to identify regions of distress using image-processing techniques. The required region properties and a decision tree for reducing selected regions of an image to conventional type, severity, and extent of pavement distress have been presented in this study. The features and decision trees have been tested on several thousand pavement images. The system of which the decision tree is part has been used successfully by ODOT since May 1994.

ACKNOWLEDGMENTS

This paper is based on research sponsored by ODOT under Grant OD-6606. The authors gratefully acknowledge the assistance of William F. Edwards, Kenneth Corns, and the engineers from the Research and Development Division at ODOT.

REFERENCES

1. Acosta, J. A. *Implementation of the Video Image Processing Technique for Evaluating Pavement Surface Distress.* M. S. thesis. Department of Civil Engineering, Case Western Reserve University, Cleveland, Ohio, 1991.
2. Figueroa, J. L., R. L. Mullen, and J. A. Acosta. A Low Cost Pavement Distress Survey and Analysis System. *Second International Symposium on Road Surface Characteristics,* Technische Universität Berlin Fachgebiet Straßenbau, 1992, pp. 528–541.
3. Chow, C. K., S. K. Hilal, and K. E. Neibuhr. X-Ray Image Subtraction by Digital Means. *IBM Journal of Research and Development,* Vol. 7, 1973, pp. 206–218.
4. Inoue, S. Video Image Processing Greatly Enhances Contrast, Quality and Speed in Polarization Based Microscopy. *Journal of Cell Biology,* Vol. 89, 1981, pp. 346–356.
5. Hung, T. S. *Picture Processing and Digital Filtering.* Springer-Verlag, Berlin, 1979.
6. Pratt, W. K. *Digital Image Processing.* John Wiley & Sons, Inc., New York, N.Y., 1978.
7. Kasturi, R., and J. F. Walkup. Nonlinear Image Restoration. *Digital Image Processing,* SPIE, Vol. 528, 1985, pp. 43–60.
8. Victor, T. T. Adaptive Filter Techniques for Digital Image Enhancement. *Digital Image Processing,* SPIE, Vol. 528, 1985, pp. 29–42.
9. Hummel, R. Image Enhancement by Histogram Transformation. *Computer Vision, Graphics, and Image Processing,* Vol. 6, 1977, pp. 184–185.
10. Pitas, I., and A. N. Venetsanopoulos. Nonlinear Order Statistic Filters for Image Filtering and Edge Detection. *Signal Processing,* Vol. 10, 1986, pp. 395–413.
11. Acosta, J. A., J. L. Figueroa, and R. L. Mullen. Low-Cost Video Image Processing System for Evaluating Pavement Surface Distress. In *Transportation Research Record 1348,* TRB, National Research Council, Washington, D.C., 1992, pp. 63–72.
12. Acosta, J. A., J. L. Figueroa, and R. L. Mullen. *Feasibility Study to Implement the Video Image Processing Technique for Evaluating Pavement Surface Distress in the State of Ohio.* Final Report No. FHWA/OH-91/010. Ohio Department of Transportation, January 10, 1992.
13. Acosta, J. A. *Pavement Surface Distress Evaluation Using Video Image Analysis.* Ph.D. dissertation. Department of Civil Engineering, Case Western Reserve University, Cleveland, Ohio, 1994.
14. Acosta, J. A., J. L. Figueroa, and R. L. Mullen. *Implementation of the Video Image Processing Technique for Evaluating Pavement Surface Distress in the State of Ohio.* Final Report No. FHWA/OH-94/005. Ohio Department of Transportation, May 1994.
15. El Sanhouri, I. M. *Computer-Based Segmentation and Interpretation of Pavement Surface Distress Images.* M.S. thesis. Massachusetts Institute of Technology, Cambridge, 1990.
16. Majidzadeh, K., and M. S. Luther. *Development and Implementation of a System for Evaluation and Maintenance and Repair Needs and Priorities.* Vol. 2. Report No. FHWA/OH-80/003. Resource International, Inc.; Ohio Department of Transportation, 1980.

Publication of this paper sponsored by Committee on Pavement Monitoring, Evaluation, and Data Storage.